

# Supporting Information

Yarwood et al. 10.1073/pnas.1706656114

## SI Materials and Methods

**Reagents.**  $\alpha$ CGRP and  $\alpha$ CGRP<sub>8-37</sub> were from Bachem. Pitstop and Dyngo are trademarks of Children's Medical Research Institute, Newcastle Innovation, and Freie Universitat Berlin and were from A. McCluskey, University of Newcastle, Newcastle, Australia. Alexa488-HA antibody was from S. Furness, Monash University, Melbourne. Sources of other reagents have been described (11–13).

**cDNAs.** A bicistronic IRES HA-CLR/myc-RAMP1 vector in pcDNA5 and DynK44E have been described (11). myc-CLR-RLuc was from M. Bouvier, Université de Montréal, Montréal. KRas-Venus, Rab5a-Venus, and Rab11-Venus were from N. Lambert, Augusta University Medical College of Georgia, Augusta, GA (12, 13).  $\beta$ ARR2-YFP was from M. Caron, Duke University, Durham, NC. The following FRET biosensor constructs were from Addgene: cytoEKAR GFP/RFP (plasmid 18680), cytoEKAR Cerulean/Venus (plasmid 18679), nucEKAR GFP/RFP (plasmid 18682) and nucEKAR Cerulean/Venus (plasmid 18681), cytoCKAR (plasmid 14870), and pmCKAR (plasmid 14862) (12, 13, 16). CytoEpac2camps was from M. Lohse, University of Wurzburg, Wurzburg, Germany, and pmEpac2camps was from D. Cooper, University of Cambridge, Cambridge, UK. pcDNA3L-His-CAMYEL was from ATCC.

**Tripartite Probes.** Sulfonated Cy5 carboxylic acid (Cy5 acid), CGRP<sub>8-37</sub>, and Span were conjugated to Chol or aspartate ethyl ester via a flexible PEG linker by standard Fmoc solid-phase peptide synthesis (SPPS) on Fmoc-PAL-PEG-PS resin (Life Technologies, 0.17 mol·g<sup>-1</sup> resin loading) (12). Fmoc deprotection reactions used 20% (v/v) piperidine in *N,N*-dimethylformamide (DMF). Coupling reactions used Fmoc-protected amino acids with *O*-(6-chlorobenzotriazol-1-yl)-*N,N,N',N'*-tetramethyluronium hexafluorophosphate (HCTU) as a coupling agent and *N,N*-diisopropylethylamine (DIPEA) as an activating agent.

**Cy5-Chol.** Cy5-Chol [Cy5-PEG4-PEG3-PEG4-Asp(OChol)-NH<sub>2</sub>] was prepared by manual SPPS using Fmoc-Asp(OChol)-OH, Fmoc-PEG4-OH, Fmoc-PEG3-OH, and Fmoc-PEG4-OH as the amino acids. After the final deprotection step, the *N* terminus was capped using a mixture of Cy5 acid, HCTU, and DIPEA in DMF, and the peptide construct was then cleaved from resin using 95:2.5:2.5 trifluoroacetic acid (TFA)/triisopropylsilane (TIPS)/water.

**CGRP<sub>8-37</sub>.** CGRP<sub>8-37</sub> [VTHRLAGLLSRGGVVKDNFVPTNVGSEAF-NH<sub>2</sub>] was prepared by manual peptide synthesis with standard Fmoc chemistry on NovaSynTG<sup>R</sup> R resin (loading 0.18 mmol·g<sup>-1</sup>, NovaBiochem). We coupled the Fmoc amino acids with 1-[bis(dimethylamino)methylene]-1*H*-1,2,3-triazolo[4,5-*b*]pyridinium 3-oxide hexafluorophosphate (HATU) and 1-hydroxy-7-azabenzotriazole (HOAt) in DMF with activation in DIPEA. Fmoc deprotection was achieved using 20% piperidine in DMF. After final *N*-deprotection, a portion of the material was cleaved from resin.

**CGRP<sub>8-37</sub>-Chol.** CGRP<sub>8-37</sub>-Chol [Ac-Asp(OChol)-PEG12-VTHRLAGLLSRGGVVKDNFVPTNVGSEAF-NH<sub>2</sub>] was prepared by coupling resin-bound CGRP<sub>8-37</sub> to Fmoc-PEG12-OH with HATU, HOAt, and DIPEA in DMF. Fmoc deprotection was achieved using 20% piperidine in DMF. Following final deprotection, the *N* terminus was capped by exposure to DIPEA and acetic anhydride in DMF, and the peptide construct was then cleaved from resin using 95:2.5:2.5 TFA/TIPS/water.

**Span-Chol.** Span-Chol [Cy5-PEG3-Asp(OChol)-PEG4-PEG3-PEG4-Span-NH<sub>2</sub>] was prepared from resin-bound Span I by manual SPPS

using Fmoc-PEG4-OH, Fmoc-PEG3-OH, Fmoc-PEG4-OH, Fmoc-Asp(OChol)-OH, and Fmoc-PEG3-OH as the amino acids. After the final deprotection step, the *N* terminus was capped using a mixture of Cy5 acid, HCTU, and DIPEA in DMF, and the peptide construct was then cleaved from resin using 95:2.5:2.5 TFA/TIPS/water.

**Purification.** Constructs were purified by reverse-phase HPLC (HPLC) (Phenomenex Luna C8 column) with 0.1% TFA/water and 0.1% TFA/ACN as solvents. Products were characterized by mass spectrometry. CGRP<sub>8-37</sub>: *m/z* (monoisotopic) C<sub>139</sub>H<sub>230</sub>N<sub>44</sub>O<sub>38</sub>; cal'd [M + 2H<sup>+</sup>] 1,563.8; obs. 1,563.9. CGRP<sub>8-37</sub>-Chol: *m/z* (monoisotopic) C<sub>199</sub>H<sub>336</sub>N<sub>46</sub>O<sub>55</sub>; cal'd [M + 3H<sup>+</sup>] 1,418.8; obs. 1,418.9. Span-Chol: *m/z* (monoisotopic) C<sub>139</sub>H<sub>220</sub>N<sub>24</sub>O<sub>31</sub>; cal'd [M + 3H<sup>+</sup>] 908.8; obs. 908.9.

**Cell Culture and Transfection.** HEK293 cells were grown in DMEM supplemented with 5% (vol/vol) FBS (37 °C, 5% CO<sub>2</sub>). Cells (2 × 10<sup>6</sup> cells, 10-cm plate) were transfected with 5 μg HA-CLR/myc-RAMP1 cDNA using polyethyleneimine (PEI, Polysciences) at a 1:6 DNA:PEI ratio. For BRET assays, cells were transfected with the following cDNAs: 1 μg myc-CLR-RLuc, 1 μg myc-RAMP1, and 4 μg KRas-Venus or 4 μg Rab5a-Venus or 4 μg Rab11-Venus or 4 μg  $\beta$ ARR2-YFP; or 3 μg HA-CLR/myc-RAMP1 and 2 μg pcDNA3L-His-CAMYEL. For single-cell FRET assays, cells in 96-well plates were transfected with 55 ng per well HA-CLR/myc-RAMP1 cDNA and 40 ng per well FRET biosensor cDNA. For experiments using dynamin WT or K44E, cells were transfected with an additional 50 ng per well of the relevant dynamin construct. For population FRET assays, cells in 10-cm plates were transfected with 2.5 μg HA-CLR/myc-RAMP1 and 2.5 μg cytoEKAR or NucEKAR. At 24–48 h after transfection, cells were plated in poly-D-lysine-coated 96-well plates. For immunofluorescence, HEK cells in 10-cm dishes were transfected with 1 μg HA-CLR/myc-RAMP1 cDNA with or without 1 μg DynK44E or 250 ng Rab5-Venus cDNA. After 24 h, cells were plated onto poly-D-lysine-coated coverslips.

**FRET.** Cells were serum-restricted overnight (0.5% vol/vol FBS) and equilibrated in HBSS at 37 °C. Single-cell FRET was analyzed using a GE Healthcare INCell 2000 Analyzer as described (12, 13, 16). Briefly, for CFP/YFP emission ratio analysis, cells were sequentially excited using a CFP filter (430/24) with emission measured using YFP (535/30) and CFP (470/24) filters, and a polychroic filter was optimized for the CFP/YFP filter pair (Quad3). Cells were imaged at 1-min intervals. Baseline emission ratio images were captured for 4 min. Cells were challenged with CGRP (1 nM, continuous) or vehicle, and images were captured for 20 min. Cells were then stimulated with positive controls (200 nM phorbol 12,13-dibutyrate for ERK; 200 nM phorbol 12,13-dibutyrate with phosphatase inhibitor mixture for PKC; 10 μM forskolin, 100 μM 3-isobutyl-1-methylxanthine, and 100 nM PGE<sub>1</sub> for cAMP) for 10 min to generate a maximal increase, and positive emission ratio images were captured for 4 min. Data were analyzed with the FIJI distribution of ImageJ. The three emission ratio image stacks (baseline, stimulated, positive control) were collated and aligned with the StackCreator script (12, 13, 16). Cells were selected, and fluorescence intensity was measured over the combined stack. Background intensity was subtracted, and FRET data were expressed as emission ratios relative to the positive controls (F/F<sub>max</sub>). Only cells that showed >10% change relative to baseline after stimulation with the positive control were considered for analysis. Population-based

FRET was measured using a PHERAstar plate reader (BMG LabTech). Cells were excited using a CFP filter (425–10 nm), and emission was measured using YFP (550–50 nm) and CFP (490–20 nm) filters. Measurements were taken every 1 min, and the CFP/YFP ratio was calculated (FRET ratio). Baseline FRET ratios were measured for 4 min before stimulation and subtracted from poststimulation FRET. Results were normalized to the maximal phorbol 12,13-dibutyrate response.

**BRET.** Cells were equilibrated in HBSS at 37 °C and incubated with the RLuc substrate coelenterazine h (NanoLight, 5  $\mu$ M, 15 min). Cells were challenged with CGRP (100 nM, continuous). BRET was measured using a PHERAstar Omega microplate reader (BMG Labtech) (12, 13). Data are presented as a BRET ratio (calculated as the ratio of the YFP signal to the *Renilla* luciferase signal) corrected for vehicle.

**Inhibitors.** Cells were preincubated for 30 min with 30  $\mu$ M each of Dy4a, Dy4a inactive (inact), PS2, and PS2 inact; 10  $\mu$ M NF449; 10  $\mu$ M NF023; 100 nM UBO-QIC; 1  $\mu$ M U73122; 100  $\mu$ M EGTA-AM (membrane permeant); or vehicle (control). Inhibitors were included throughout the assays. For studies of tripartite antagonists, cells were incubated for 30 min with CGRP<sub>8–37</sub>, CGRP<sub>8–37</sub>-Chol, PEG-Biotin-Chol (30 nM–10  $\mu$ M), or vehicle; washed; and then challenged with CGRP immediately after washing or after 4 h of recovery.

**Cell-Surface ELISA.** Cells were exposed to CGRP (100 nM, 0–120 min, 37 °C) or vehicle, washed with DMEM at pH 2.5, and fixed in 3.7% paraformaldehyde in Tris-buffered saline for 30 min. Cells were incubated in blocking buffer [1% skim milk powder in 0.1 M NaHCO<sub>3</sub>, 4 h room temperature (RT)] and incubated with anti-HA (1:5,000) or anti-myc (9E10) (1:10,000) antibodies (overnight 4 °C). Cells were washed and incubated with anti-mouse horseradish peroxidase-conjugated antibody (1:2,000, 2 h RT). Cells were stained using the SIGMAFAST OPD substrate (Sigma). Absorbance at 490 nm was measured using the EnVision plate reader (PerkinElmer). Values were normalized to HEK293 cells transfected with pcDNA3. Ligand-induced internalization was calculated as a percentage of the signal in vehicle-treated cells.

**Immunofluorescence and Confocal Microscopy.** HEK-HA-CLR/myc-RAMP1 cells were treated with CGRP (100 nM, 15 min) and fixed (4% paraformaldehyde in PBS, 20 min on ice). Cells were washed with PBS (3  $\times$  10 min), permeabilized, and blocked using 5% normal horse serum and 0.1% saponin in PBS (30 min, RT). Cells were incubated with antibodies to HA (rat monoclonal, 1:1,000; Roche) and EEA1 (mouse monoclonal, 610457, 1:200; BD Biosciences) (overnight, 4 °C). Primary antibodies were detected using secondary antibodies conjugated to Alexa Fluor 488 or 568 (1:500, 1 h, RT; ThermoFisher). Coverslips were mounted onto slides using ProLong Diamond Antifade Mountant (ThermoFisher). Cells were observed using a Leica TCS SP8 Confocal Laser Scanning Microscope and a HCX PL APO 63 $\times$  (N.A. 1.40) oil objective. Images (1,024  $\times$  1,024 resolution and 16-bit depth) were captured as *z* stacks.

**Cy5-Chol and CLR Internalization.** HEK293 cells were plated onto poly-L-lysine eight-well chamber slides and grown to 50% confluence. Cells were transfected with HA-CLR/myc-RAMP1 using Eugene HD (Promega). After 24 h, cells were transferred to serum-free DMEM supplemented with 1 $\times$  antibiotic-antimycotic (ThermoFisher Scientific). Cells were incubated with Cy5-Ethyl Ester Control or Cy5-Chol (200 nM, 60 min, 37 °C) and washed. Cells were then incubated with Alexa Fluor 488-labeled anti-HA monoclonal antibody (clone 12CA5, 10  $\mu$ g/mL, 40 min, RT in HBSS supplemented with 10 mM glucose and 0.1% BSA, pH 7.4) and washed. Live cells were imaged by

confocal microscopy. Cells were stimulated with 50 nM CGRP 3 h after the initial probe addition. Images were obtained using a Leica TCS SP8 Confocal Laser Scanning Microscope and a HCX PL APO 63 $\times$  (N.A. 1.40) oil objective in humidified, temperature-controlled conditions (37 °C). Images were acquired at 512  $\times$  512 with a pinhole set to 0.5 Airy units, capturing Cy5 (ex, 633; em, 650  $\pm$  20 nm) and Alexa488-HA antibody conjugate (ex, 488; em, 520  $\pm$  20 nm) and bright-field channels. Image acquisition settings were consistent for Cy5-Chol and Cy5-Ethyl Ester fluorescence detection. Images were annotated with FIJI (v 1.48v) Image J analysis software. Pixel intensities over distance were measured by plotting pixel intensity profiles. The distribution of Cy5-Chol, Cy5-Ethyl Ester, and Alexa488-labeled HA-CLR was analyzed by Mander's Coefficient (25) to indicate overlap of pixels as a representation of colocalization for 6–14 cells, acquired from four separate experiments. Videos were processed by deconvolution (Nyquist theorem).

**Animals.** The Institutional Animal Care and Use Committees of Monash University and the University of Sydney approved all studies. Rats (Sprague-Dawley, males, 3–8 wk) and mice (C57BL/6, males, 6–10 wk) were from the Monash Animal Research Platform and the Animal Resources Centre, Western Australia. Animals were maintained in a temperature-controlled environment with a 12 h light/dark cycle and free access to food and water. Animals were killed by anesthetic overdose and thoracotomy.

**Spinal Cord Slices.** Parasagittal slices (340–400  $\mu$ m) were prepared using a vibratome from the lumbar region of the rat spinal cord in ice-cold artificial CSF (sACSF) (in mM: 100 sucrose, 63 NaCl, 2.5 KCl, 1.2 NaH<sub>2</sub>PO<sub>4</sub>, 1.2 MgCl<sub>2</sub>, 25 glucose, 25 NaHCO<sub>3</sub>; 95% O<sub>2</sub>/5% CO<sub>2</sub>) (26). Slices were transferred to *N*-Methyl-D-Glutamine (NMDG)-based recovery ACSF (rACSF) (in mM: 93 NMDG, 93 HCl, 2.5 KCl, 1.2 NaH<sub>2</sub>PO<sub>4</sub>, 30 NaHCO<sub>3</sub>, 20 Hepes, 25 glucose, 5 Na ascorbate, 2 thiourea, 3 Na pyruvate, 10 MgSO<sub>4</sub>, 0.5 CaCl<sub>2</sub>; 95% O<sub>2</sub>/5% CO<sub>2</sub>, 15 min, 34 °C). Slices were transferred to normal ACSF (in mM: 125 NaCl, 2.5 KCl, 1.25 NaH<sub>2</sub>PO<sub>4</sub>, 1.2 MgCl<sub>2</sub>, 2.5 CaCl<sub>2</sub>, 25 glucose, 11 NaHCO<sub>3</sub>; 95% O<sub>2</sub>/5% CO<sub>2</sub>) containing 10  $\mu$ M MK-801 (45 min, 34 °C), then maintained at RT.

**Electrophysiology.** Slices were transferred to a recording chamber and superfused with ACSF (2 mL $\cdot$ min<sup>-1</sup>, 36 °C). Dodt-contrast optics were used to identify large (capacitance  $\geq$  20 pF), putative CLR- and NK<sub>1R</sub>-positive neurons in lamina I based on their location, size, and fusiform shape. Slices were preincubated with Dy4 or Dy4 inact (30  $\mu$ M, 0.03% DMSO) for 10 min before recording or were preincubated with CGRP<sub>8–37</sub>-Chol or CGRP<sub>8–37</sub> (1  $\mu$ M, 0.01% DMSO) for 60 min, washed, and incubated in antagonist-free ACSF for a further 60 min before recording. Spontaneous currents were recorded in cell-attached configuration (Multiclamp 700B; Molecular Devices), sampled at 10 kHz, high pass-filtered at 1 Hz, and capacitively coupled action potential events were analyzed using Axograph X, V 1.4.4 (Axograph) (26). Patch electrodes (resistance, 2.5–3.5 M $\Omega$ ) contained KMES-based internal solution (in mM: 105 KMES, 20 NaCl, 5 Hepes, 10 BAPTA, 1.5 MgCl<sub>2</sub>, 4 MgATP, 0.4 NaGTP; 0.1% biocytin; 285–295 mosmol $\cdot$ L<sup>-1</sup>) to facilitate subsequent recordings of action potential properties in whole-cell configuration. Recordings were made in the presence of CNQX (6-cyano-7-nitroquinoxaline-2,3-dione, 10  $\mu$ M, AMPA/kainate receptor antagonist), picrotoxin (100  $\mu$ M, GABA<sub>A</sub> receptor antagonist), strychnine (0.5  $\mu$ M, glycine and acetylcholine receptor antagonist), and AP5 [(2*R*)-amino-5-phosphonovaleric acid; 2*R*-amino-5-phosphonopentanoate, 100  $\mu$ M, NMDA receptor antagonist] to minimize presynaptic effects on action potential properties. Slices were challenged by superfusion with CGRP

(1  $\mu\text{M}$ , 2 min). CGRP-stimulated slices were challenged with SP (1  $\mu\text{M}$ , 2 min) at the end of the experiment to confirm coexpression of CGRP and SP receptors. Recordings were sampled at 10 kHz and filtered with a high pass filter at 1 Hz, and firing rate was measured in 2-min interval bins. At the end of cell-attached recording, whole-cell recordings were made in current-clamp mode to confirm retention of normal action potential firing. Data were only included in the analysis if cells had action potential amplitudes that were  $\geq 50$  mV above threshold to ensure viable neurons were included. Cells were filled with biocytin, and sections were processed to confirm CLR expression by immunofluorescence. The firing rate for each cell was normalized to the response at 2–4 min, which was not significantly different between groups. The firing time was determined as the duration of the response to last action potential.

**CLR Localization.** Spinal cord slices (400  $\mu\text{m}$ ) were incubated with CGRP (1  $\mu\text{M}$ , 5 min), fixed in paraformaldehyde (4 h, RT), cryoprotected, and processed to localize CLR-IR and NeuN-IR as described (27). The z stack images of the CLR-IR neurons in lamina I of the dorsal horn were collected with a Leica TCS SP8 Confocal Laser Scanning Microscope and a HCX PL APO 63 $\times$  (N.A. 1.40) oil objective. For quantification of CLR endocytosis, z stacks were imported into Image J. The border of the neuronal soma was defined by NeuN-IR. CLR-IR within 5 pixels (0.5  $\mu\text{m}$ ) of the soma border was defined as the plasma membrane-associated receptor, while the remainder was defined as a cytoplasmic receptor, as described (12). The ratio of plasma membrane to cytosolic CLR-IR was determined.

**Nociception.** Mice were acclimatized to the apparatus for 1–2 h on 2 successive days before the experiments. Mechanical allodynia and hyperalgesia were assessed by paw withdrawal to stimulation of the plantar surface of the hindpaw with graded von Frey filaments (12). Baseline scores were recorded in triplicate 1 d before the studies. Mice were sedated (5% isoflurane), and capsaicin (5  $\mu\text{g}$ ), CFA (2  $\text{mg}\cdot\text{mL}^{-1}$ ), or vehicle (capsaicin, 20% ethanol, 10% Tween 80, 70% saline; CFA, saline) was injected s.c. into the plantar surface of the left hindpaw (10  $\mu\text{L}$ ). von Frey scores (left and right paws) were measured for 1–4 h post-

capsaicin and 36–40 h post-CFA. Results are expressed as percent preinjected values. For assessment of nocifensive behavior, mice were sedated and formalin (4%, 10  $\mu\text{L}$ ) was injected s.c. into the plantar surface of the left hindpaw. Mice were placed in a Perspex container, and nocifensive behavior (flinching, licking, biting of the injected paw) was recorded for 60 min. The total number of nocifensive events was subdivided into acute (I, 0–10 min) and tonic (II, 10–60 min) phases. Investigators were blinded to test agents. Intrathecal injections (5  $\mu\text{L}$ , L3/L4) were made into conscious mice. CGRP<sub>8–37</sub> (10  $\mu\text{M}$ ), CGRP<sub>8–37</sub>-Chol (10  $\mu\text{M}$ ), Span (50  $\mu\text{M}$ ), or Span-Chol (50  $\mu\text{M}$ ) was injected intrathecally 3 h before injection of capsaicin or formalin, or 36 h after CFA.

**Spinal Neuron Culture.** Superficial dorsal horn neurons were prepared from 1- to 2-d-old neonatal rats. The spinal cord was exposed by laminectomy and the superficial dorsal horn dissected (approximately lamina I–III). Tissue was incubated in HBSS containing papain (20 U/mL, 30 min, RT; Worthington Bio-Chemical). Tissue was rinsed in HBSS and mechanically dissociated by gently triturating with plastic pipettes. The cell suspension was placed in Neurobasal-A medium containing FBS (2.5%), heat-inactivated horse serum (2.5%), GlutaMax Supplement (2 mM), and B-27 (2%) (ThermoFisher). The suspension was centrifuged (500 g, 5 min) and plated onto 12 mm poly-L-lysine-coated coverslips. Cells were cultured for 6–8 d before the study (37 °C, 5% CO<sub>2</sub>). [Ca<sup>2+</sup>]<sub>i</sub> was measured in individual spinal neurons using Fura-2AM (28). Neurons were challenged with CGRP (1  $\mu\text{M}$ ), followed by KCl (50 mM). In some experiments, neurons were pretreated with CGRP<sub>8–37</sub> (1  $\mu\text{M}$ , 30 min).

**Statistics.** Results are presented as mean  $\pm$  SEM. Differences were assessed using Student's *t* test for two comparisons. For multiple comparisons, differences were assessed using one- or two-way ANOVA followed by Dunnett's multiple comparison test (fluorophore colocalization, nociception), Tukey's multiple comparison test (single-cell FRET), Sidak's multiple comparisons test (BRET, population FRET, average firing rate of spinal neurons), or Dunn's multiple comparisons test (duration of firing response of spinal neurons).

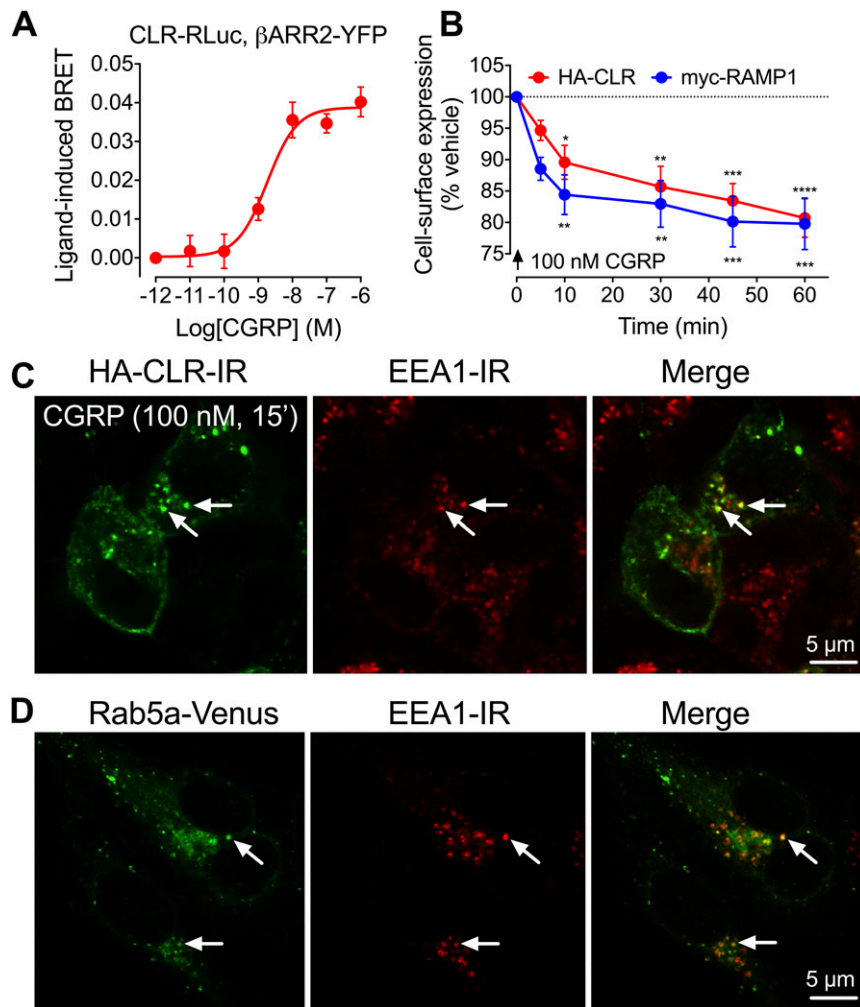


**Fig. S1.** CLR endocytosis. (A) BRET assays of CLR-RLuc8 and  $\beta$ ARR2-YFP in HEK cells. (B) Cell-surface HA-CLR and myc-RAMP1 in HEK cells.  $n = 3$  experiments.  $*P < 0.05$ ,  $**P < 0.01$ ,  $***P < 0.001$ ,  $****P < 0.0001$  to vehicle control. ANOVA, Dunnett's test. (C) Confocal images of HA-CLR-IR and EEA1-IR in HEK cells. (D) Confocal images of Rab5a-Venus and EEA1-IR in HEK cells.

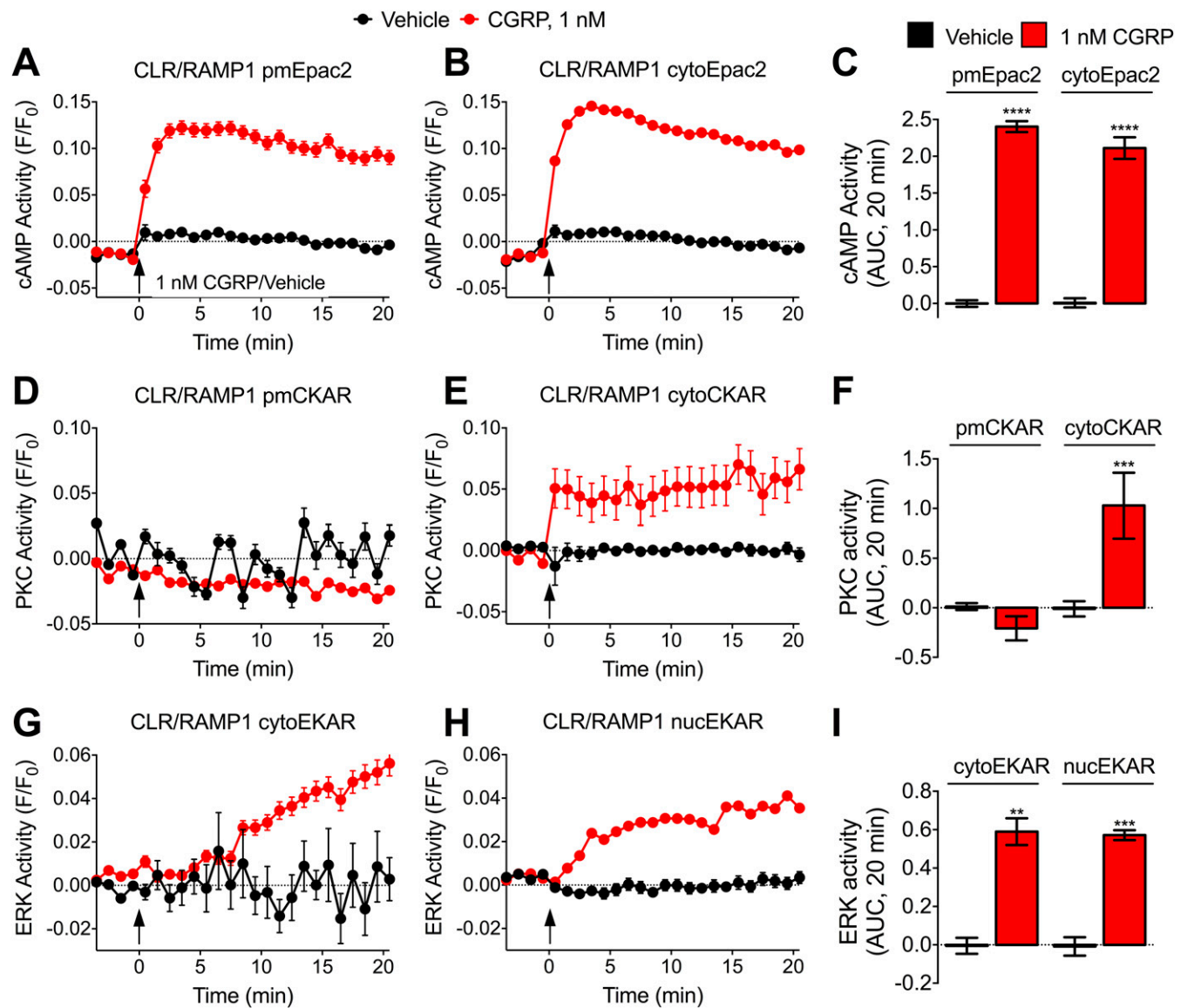


**Fig. S2.** CLR compartmentalized signaling. FRET assays of CGRP-induced activation of plasma membrane (pmEpac2) and cytosolic (cytoEpac2) cAMP (A–C), plasma membrane (pmCKAR) and cytosolic (cytoCKAR) PKC (D–F), and cytosolic (cytoEKAR) and nuclear (nucEKAR) ERK (G–I) in individual HEK-HA-CLR/myc-RAMP1 cells. (A, B, D, E, G, and H) Kinetics. (C, F, and I) Area under curve (AUC).  $n = 82\text{--}354$  cells,  $n = 3$  experiments.  $**P < 0.01$ ,  $***P < 0.001$ ,  $****P < 0.0001$  to vehicle. ANOVA, Sidak's test.

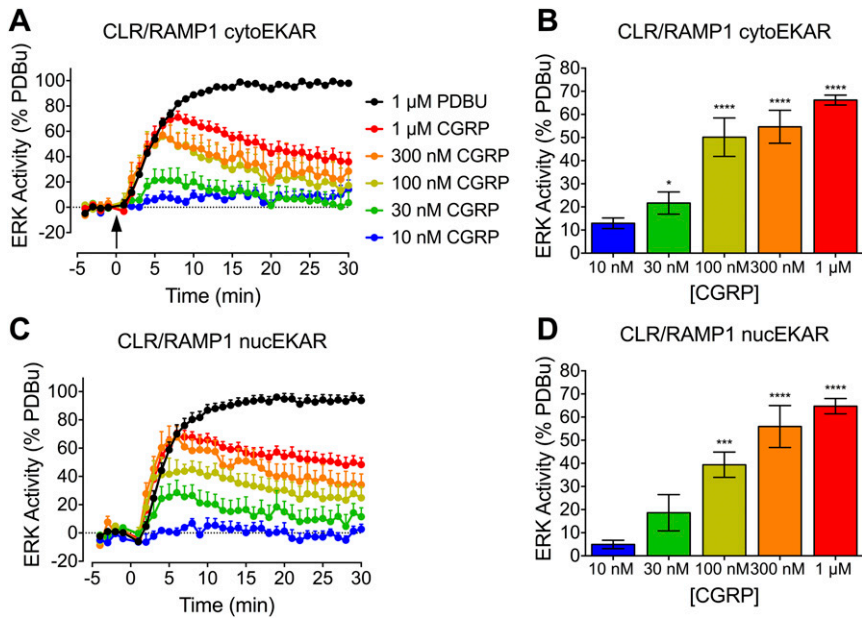
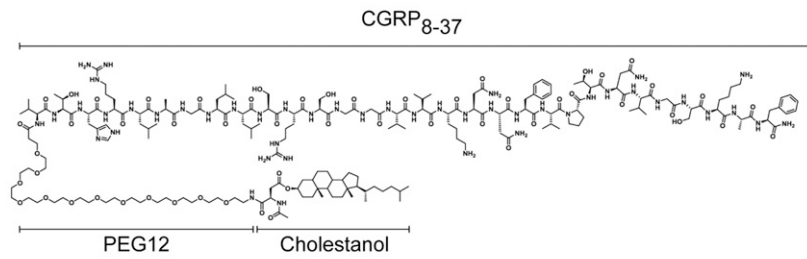


**Fig. 53.** CLR compartmentalized signaling. FRET assays of CGRP-induced activation of cytosolic (cytoERKAR, *A* and *B*) and nuclear (nucERKAR, *C* and *D*) ERK (*G*–*I*) in populations of HEK-HA-CLR/myc-RAMP1 cells.  $n = 4–9$  experiments.  $*P < 0.05$ ,  $***P < 0.001$ ,  $****P < 0.0001$  to vehicle. ANOVA, Sidak's test.

**A** CGRP<sub>8-37</sub>-PEG12-Cholestanol (C<sub>199</sub>H<sub>336</sub>N<sub>46</sub>O<sub>55</sub>)



**B** LC Profile at 214 nm

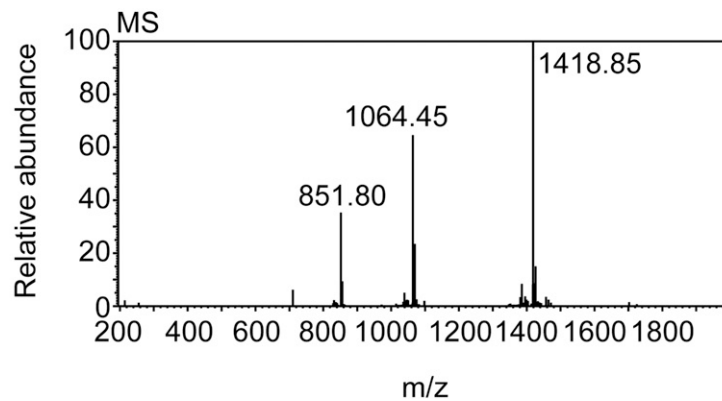
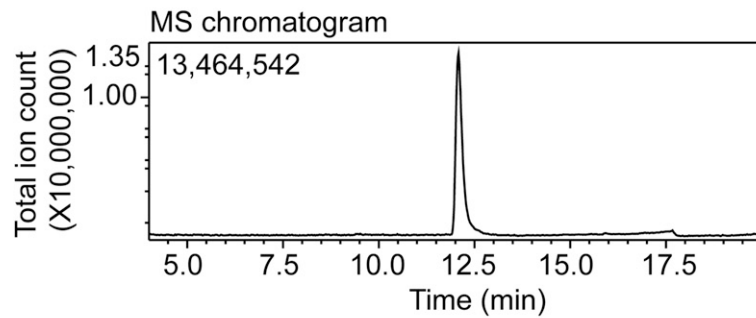
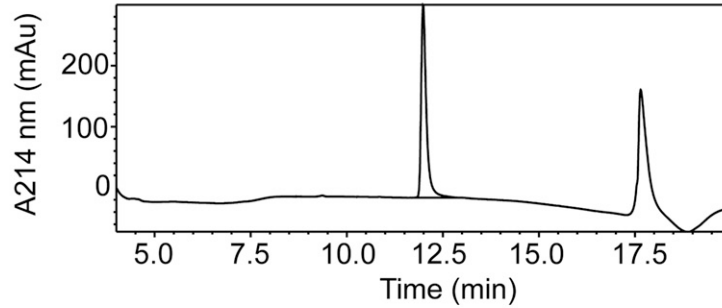


**Fig. S4.** Tripartite probes. (A) Structure of CGRP<sub>8-37</sub>-Chol. (B) LCMS analysis of CGRP<sub>8-37</sub>-Chol. Peaks at 17.5 min in the LC profile reflect changes in the baseline of the LC-MS gradient, as confirmed by injection of a blank solvent sample using the same method.

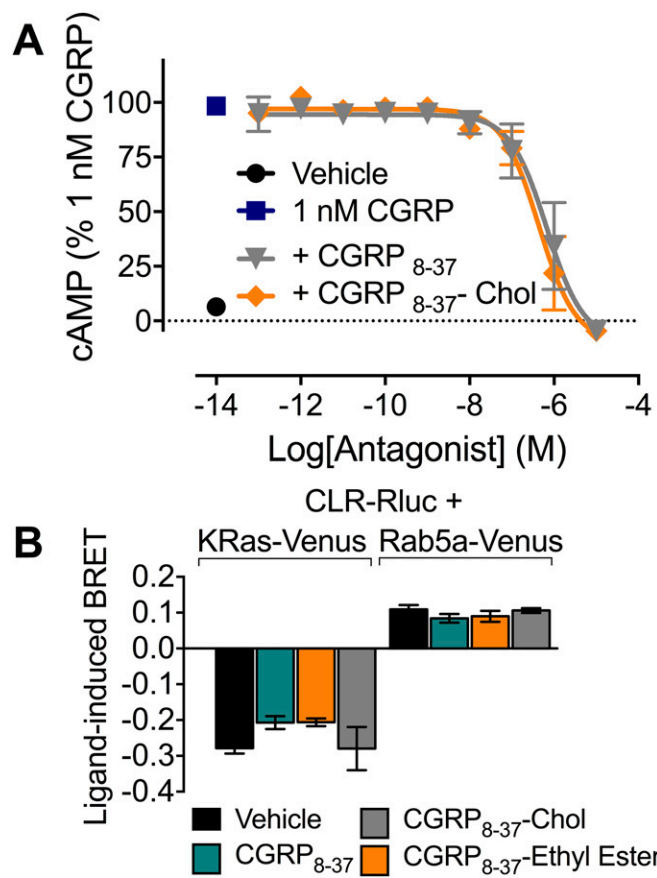


**Fig. S5.** Tripartite antagonism of CLR signaling and trafficking. (A) cAMP signaling in HEK-HA-CLR/myc-RAMP1 cells. (B) BRET assays of CLR-RLuc8 and KRas-Venus or Rab5a-Venus proximity in HEK cells. BRET was measured 4 h after 30-min pulse incubation with antagonists.  $n = 3$  experiments.



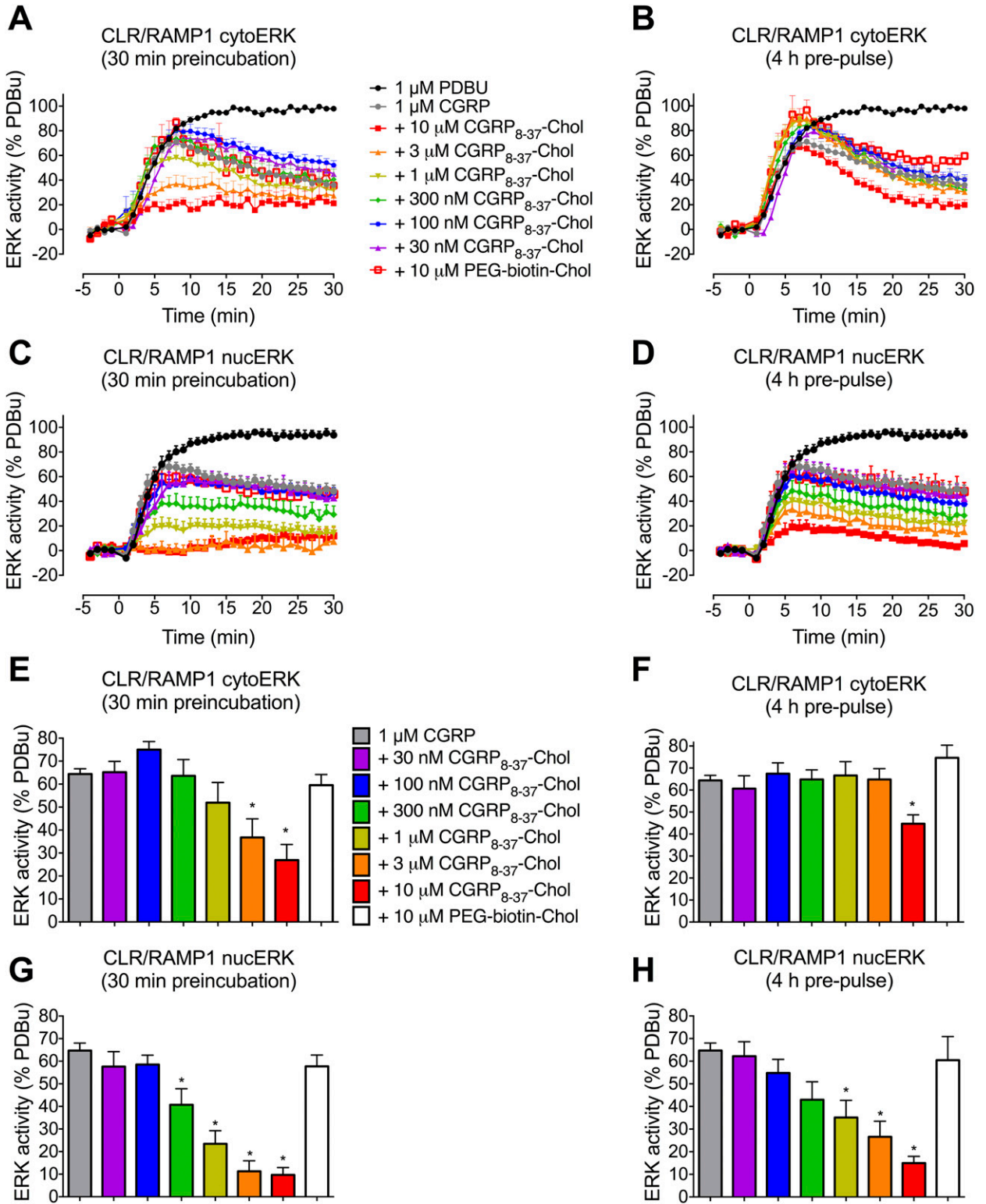


**Fig. S6.** Tripartite antagonism of CLR. ERK activity was assessed in populations of HEK-HA-CLR/myc-RAMP1 cells expressing FRET biosensors for cytosolic ERK (A, B, E, and F, cytoERKAR) and nuclear (C, D, G, and H, nucERKAR) ERK. Cells were preincubated with vehicle, CGRP<sub>8-37</sub>-Chol or PEG-Chol for 30 min and washed. CGRP-stimulated ERK activity was assessed immediately after washing (A, C, E, and G, 30 min preincubation) or 4 h after washing (B, D, F, and H, 4 h prepulse).  $n = 3-9$  experiments.  $*P < 0.05$  to vehicle. ANOVA, Sidak's test.

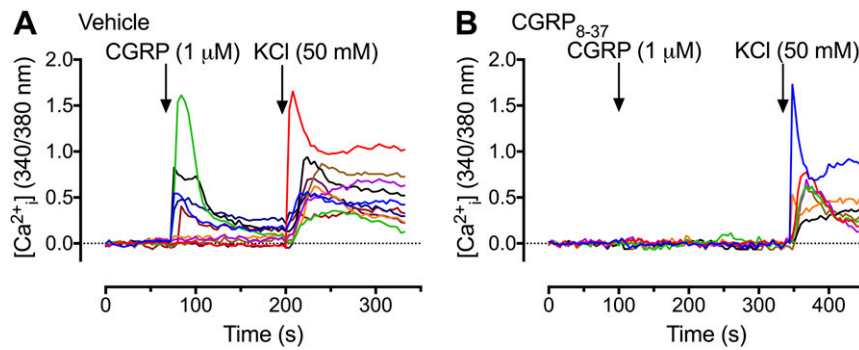


**Fig. 57.** CGRP  $\text{Ca}^{2+}$  signaling in spinal neurons. Neurons were preincubated with vehicle (A) or CGRP<sub>8-37</sub> (B) and were then challenged with CGRP. Each trace is from a single neuron.

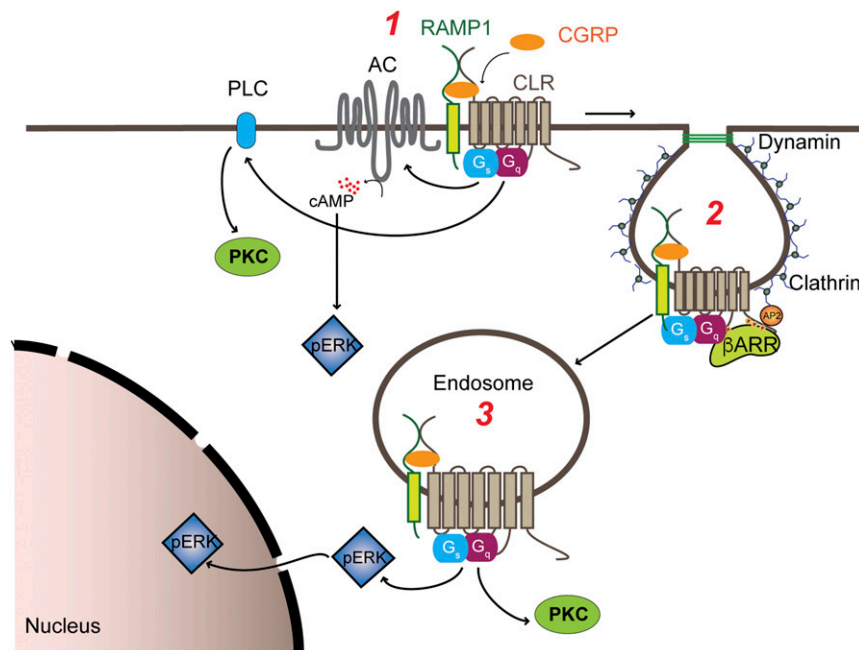
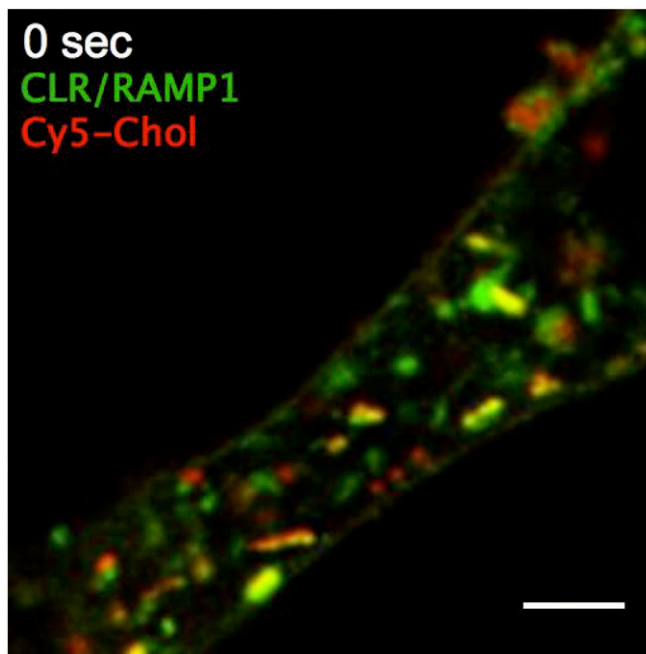


**Fig. 58.** CGRP signaling at the plasma membrane and in endosomes. (1) At the plasma membrane, CLR couples to  $\text{G}\alpha_q$ , leading to activation of phospholipase C $\beta$  (PLC) and cytosolic PKC. Plasma membrane CLR also couples  $\text{G}\alpha_s$ , leading to activation of adenylyl cyclase (AC), generation of cAMP, and stimulation of cytosolic ERK. (2) Activated CLR/RAMP1 undergoes  $\beta$ ARR-, clathrin-, and dynamin-dependent endocytosis. (3) In endosomes, CLR couples to  $\text{G}\alpha_q$ , which activates PKC in the cytosol, and  $\text{G}\alpha_s$ , which activates ERK that translocates to the nucleus.



**Movie S1.** Live cell imaging of CLR and Cy5-Chol. HEK293 cells were transfected with CLR/RAMP-1. HA-CLR was detected by labeling live cells with HA-Alexa488 antibody conjugate (green channel). Cells were incubated with Cy5-Chol (200 nM). Cells were stimulated with CGRP (50 nM, 30 min) to induce CLR endocytosis. The video was captured on a Leica TCS SP8 Confocal Laser Scanning Microscope and a HCX PL APO 63 $\times$  (N.A. 1.40) oil objective with a 0.5-AU pinhole (1,800 Hz bidirectional scanning). Stacks of 3  $\times$  z sections (0.3  $\mu$ m per section) were captured every 500 ms. Videos were processed with Huygen's Deconvolution to reduce noise. (Scale bar, 2  $\mu$ m.)

[Movie S1](#)